Acta Crystallographica Section B
Structural Science
ISSN 0108-7681

$CaSeO_4 \cdot 0.625H_2O$ – water channel occupation in a bassanite related structure

Susanne Fritz,[a] Horst Schmidt,[a] Iris Paschke,[a] Oxana V. Magdysyuk,[b] Robert E. Dinnebier,[b] Daniela Freyer[a]* and Wolfgang Voigt[a]

[a]TU Bergakademie Freiberg, Institut für Anorganische Chemie, Leipziger Strasse 29, D-09596 Freiberg, Germany, and [b]Max-Planck-Institut für Festkörperforschung, Heisenbergstrasse 1, D-70569 Stuttgart, Germany

Correspondence e-mail: daniela.freyer@chemie.tu-freiberg.de

Received 9 February 2011
Accepted 16 May 2011

Calcium selenate subhydrate, $CaSeO_4 \cdot 0.625H_2O$, was prepared by hydrothermal conversion of $CaSeO_4 \cdot 2H_2O$ at 463 K. From the single crystals obtained in the shape of hexagonal needles, 50–300 μm in length, the crystal structure could be solved in a trigonal unit cell with space group $P3_221$. The cell was confirmed and refined by high-resolution synchrotron powder diffraction. The subhydrate was characterized by thermal analysis and Raman spectroscopy.

1. Introduction

Existing phases in the $CaSeO_4 \cdot H_2O$ system are often compared with phases in the $CaSO_4 \cdot H_2O$ system. In analogy to the stoichiometries of the calcium sulfates the three phases $CaSeO_4 \cdot 2H_2O$, $CaSeO_4 \cdot 0.5H_2O$ and $CaSeO_4$ have been reported (Krüger & Abriel, 1991; Simon *et al.*, 1963; Snyman & Pistorius, 1963; Selivanova & Shneider, 1958; Fernández-González *et al.*, 2006).

The dihydrate, or selenate gypsum, is the stable phase in aqueous solutions up to the boiling point of the saturated solution. Its solubility is more than 20 times higher than that of gypsum (Selivanova & Shneider, 1959; Meyer & Aulich, 1928; Nishimura & Hata, 2007). Gypsum and selenate gypsum are very similar in *e.g.* crystal structures and twinning properties, and they can form solid solutions with each other (Krüger & Abriel, 1991; Pedersen & Semmingsen, 1982; Fernández-González *et al.*, 2006).

Selivanova & Shneider (1958) investigated the dehydration behavior of calcium selenate dihydrate by means of TG (thermogravimetry)/DTA (differential thermal analysis). They found the heating curve to be analogous to that of gypsum up to 873 K. They observed the intermediate formation of a hemihydrated phase as well as two different anhydrous phases before the decomposition of the salt. On the contrary Fernández-González *et al.* (2006) reported that during thermogravimetric analysis of the selenate gypsum the calcium selenate hemihydrate was formed at 440 K and remained stable up to unusually high temperatures close to the decomposition of the calcium selenate. (The dehydration behavior of sulfate gypsum is well known; *e.g.* thermal analysis can be found in Kuntze, 1965, Berthold *et al.*, 2011, Murat & Comel, 1971, and Borrachero *et al.*, 2008.)

As for the sulfate gypsum (Jacques *et al.*, 2009; Abriel & Reisdorf, 1990), the temperature-dependent phase transitions of selenate gypsum were investigated with temperature-controlled X-ray diffraction experiments. Snyman & Pistorius (1963) reported the selenate gypsum and the hemihydrated phase to be isomorphous to the corresponding sulfates. However, for the anhydrous phase, obtained by heating the selenate gypsum at 573 K for 3 h, the diffraction patterns were

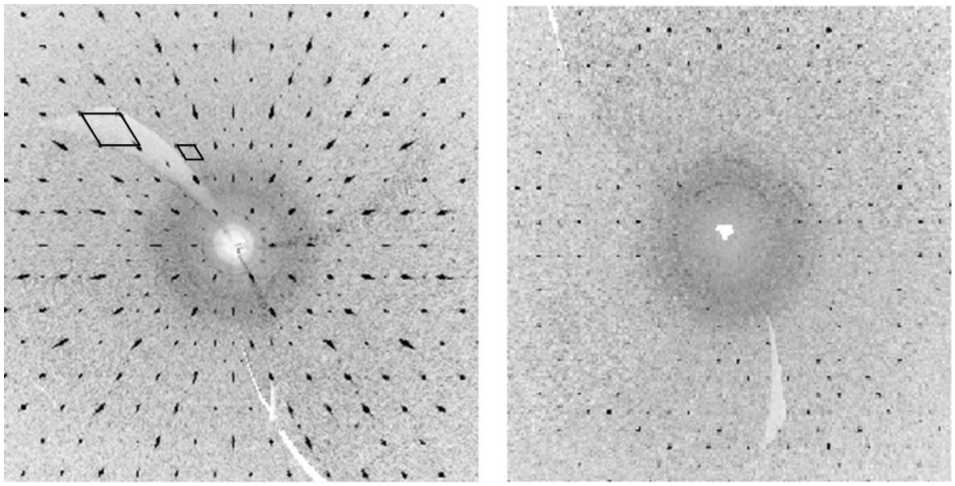

(*a*) (*b*)

Figure 1
Reconstructed reciprocal space planes of calcium selenate subhydrate; (*hk*0) with small (larger rhombohedra) and large (smaller rhombohedra) trigonal unit cell sketched in (*a*), and (*hk*1) (*b*).

completely different from $CaSO_4$ (AII). Crichton *et al.* (2010) confirmed the work of Snyman & Pistorius (1963) and identified the anhydrous phase to be of the monazite type. During the dehydration of the selenate gypsum they observed two other phases, which they suggest to be the hemiyhdrate and γ-$CaSeO_4$. There is no evidence in the literature that an anhydrous selenate phase similar in structure to the insoluble calcium sulfate anhydrite (AII) exists. Structure determination from single crystals, especially for the hemihydrated phase, and characterization of the pure isolated phases are also lacking.

So far, the existence of selenate phases analogous to the calcium sulfate subhydrates[1] with water contents somewhat higher than 0.5 has not been reported in the literature. For the sulfate system Kuzel & Hauner (1987), Bezou *et al.* (1990) and Oetzel (1999) report that the sulfate subhydrates are reversibly formed from the hemihydrate at higher relative humidity. Structure investigations resulted in monoclinc (Bezou *et al.*, 1995; Rinaudo & Boistelle, 1991; Bushuev & Borisov, 1982*a*) as well as trigonal space groups (Abriel, 1983; Abriel & Reisdorf, 1990; Kuzel & Hauner, 1987) where the water molecules are statistically arranged within the water channels. Subsequent papers dealing in more detail with the structure (Schmidt, 2011) and the water content in correlation with the formation conditions (Paschke, 2011*b*) of the subhydrates in the sulfate system are in preparation.

Despite the many investigations, not everything is as clear as desired about a system with such industrial importance as the calcium sulfate–water system. New information on structure and stability in analogous systems can be helpful for further discussions. For that we adapted for the selenate system a method established to synthesize α-$CaSO_4{\cdot}0.5H_2O$. A pure phase was obtained, but the experiments showed that contrary to the sulfate system a water content higher than 0.5 is stabilized in the selenate system. The synthesis and structure determination of this calcium selenate subhydrate are reported in the current paper. The structure is presented with particular respect to the structure of the water channels and observed differences to the sulfate system. The structure determination of calcium selenate subhydrate is a helpful step for discussions about the structure modifications of calcium sulfate hemihydrate ($CaSO_4{\cdot}0.5H_2O$, bassanite) occurring when transforming to the calcium sulfate subhydrates ($CaSO_4{\cdot}xH_2O$, $0.5 < x \leq 0.8$) at high relative humidity.

2. Experimental

2.1. Synthesis and characterization

Calcium selenate subhydrate was obtained by hydrothermal synthesis. Calcium selenate dihydrate (selenate gypsum) was used as the starting material. The selenate gypsum was crystallized at room temperature from aqueous solution containing 0.25 mol l^{-1} of analytical grade Na_2SeO_4 and $Ca(NO_3)_2{\cdot}4H_2O$ (Fluka, p.a.) each. The phase was identified by X-ray powder diffraction (JCPDS No.40-235) and the purity was confirmed by TG/DTA and Raman spectroscopy (free of nitrate vibrations).

For the synthesis of calcium selenate subhydrate 3.3 g of selenate gypsum and 15 g of deionized water were placed in a 30 ml Teflon cup in a TiPd autoclave. The autoclave was kept at a constant temperature of 190 $\pm$ 1 K within a metal block thermostat for 16 h. During that time the autoclave was rotated around its own axis with alternating directions for the phase equilibration. Separation of the solid phase from the solution was carried out at the same temperature using a high-temperature centrifuge of special construction that allows direct transfer of the autoclave from the block thermostat into the centrifuge. The entire equipment is described in detail by Freyer & Voigt (2004). After phase separation the hot autoclaves were instantly opened, the product taken out and kept in a dessicator over silica at room temperature for at least 2 d.

The X-ray powder diffraction patterns for phase identifications were collected with a Bruker D 5000 $\theta - \theta$ diffractometer (Cu $K\alpha$ radiation). Thermal analyses were carried out using a DTA/TG 22 of Seico Instruments (reference substance Al_2O_3, open platinum crucibles, nitrogen flow 300 ml min^{-1},

[1] The term "subhydrate" is used for phases with water contents not exactly corresponding to the hemihydrate of 0.5.

Table 1
Experimental details for the X-ray data collection and crystallographic parameters for the single-crystal structure of $CaSeO_4 \cdot 0.625H_2O$ at 296 and 100 K.

For all structures: $CaH_{1.25}O_{4.625}Se$, M_r = 194.30, trigonal, $P3_221$, Z = 24. Experiments were carried out with Mo $K\alpha$ radiation using a Bruker X8 Kappa Apex2 diffractometer. Absorption was corrected for by multi-scan methods, *SORTAV* (Blessing, 1995). Refinement was on 258 parameters with 5 restraints. H atoms were treated by a mixture of independent and constrained refinement. The absolute structure was obtained using Flack (1983).

	296 K	100 K
Crystal data		
a, c (Å)	14.1683 (2), 13.4241 (2)	14.1035 (7), 13.3622 (10)
V (Å^3)	2333.68 (6)	2301.8 (2)
μ (mm^{-1})	10.85	10.85
Crystal size (mm)	0.1 × 0.04 × 0.01	0.1 × 0.04 × 0.01
Data collection		
T_{min}, T_{max}	0.695, 0.748	0.695, 0.748
No. of measured, independent and observed [$I > 2\sigma(I)$] reflections	25 493, 3584, 2801	31 621, 3531, 3005
R_{int}	0.054	0.044
Refinement		
$R[F^2 > 2\sigma(F^2)]$, $wR(F^2)$, S	0.033, 0.074, 1.06	0.033, 0.082, 1.18
No. of reflections	3584	3531
$\Delta\rho_{max}$, $\Delta\rho_{min}$ (e Å^{-3})	0.57, −0.59	0.81, −1.13
Flack parameter	0.551 (14)	0.426 (15)

heating rate 5 K min^{-1}). Raman spectra were recorded using a FT–Raman spectrometer RFS 100/S (Bruker Optik GmbH) with a 1064 nm Nd:YAG laser and a liquid nitrogen-cooled germanium detector. SEM pictures were taken with a TESCAN Vega 5130 SB (20 kV accelerating voltage), after coating the samples with gold.

2.2. Single-crystal diffraction, structure solution and refinement

Single crystals of calcium selenate subhydrate, obtained by hydrothermal conversion of calcium selenate dihydrate, were selected under the microscope in polarized light. The crystals were translucent and colourless. Most of the crystals were too small for diffraction experiments. A needle-shaped crystal with the dimensions 0.1 × 0.01 × 0.01 mm was mounted in a glass capillary for X-ray analysis.

Data collection was performed at room temperature (293 K) and at 100 K with a Bruker X8 kappa diffractometer and an APEXII detector. *APEX*2 software (Bruker AXS, 2005) was used for indexing, integration and data reduction; *SHELXS*97 and *SHELXL*97 (Sheldrick, 2008) were used for structure solution and refinement.

The reciprocal space shows a trigonal symmetry of strong reflections but also very weak superstructure reflections in the middle between the strong ones, evident from the reciprocal space maps (*hk*0) and (*hk*1) in Fig. 1. Since there has been much controversial discussion about the nature of the calcium sulfate subhydrates as well as the trigonal and monoclinic structures of calcium sulfate hemi- and subhydrates, we will give some detail about the structure solution and refinement procedure of the calcium selenate subhydrate.

All strong reflections with intensities $I/\sigma(I) \geq 250$ could be indexed by a trigonal unit cell with a = 7.0886 and c = 6.712 Å. Space-group determination was performed using *XPREP* (Sheldrick, 2008); structure solution and refinement resulted in a crystal structure in the space group $P3_221$. This cell is very similar in lattice parameters to the trigonal cell suggested from X-ray powder diffraction for the selenate hemihydrate (Snyman & Pistorius, 1963) as well as to former trigonal/hexagonal structure solutions of calcium sulfate hemihydrate (Gallitelli, 1933; Bushuev & Borisov, 1982*b*; Abriel & Nesper, 1993). The solution is reasonable. The statistical R values are small ($R_1 > 4\sigma$ = 0.013, wR_2all = 0.027), the goodness of fit is 1.084 and the anisotropic displacement parameters are as expected. Disadvantages include split positions for some O atoms and an occupancy of 0.67 for channel water O atoms, while not all of the possible positions are physically reasonable. Furthermore, the measured weak reflections cannot be explained with this solution. In spite of the insufficiency of this solution the coordinates and anisotropic temperature parameters are given in the supporting material[2] for comparison with other structures. This can be useful for the discussion of water occupation of the channels in subhydrates and bassanite-type structures. However, in order to take the weak reflections into account larger unit cells have to be applied.

There were two possible solutions in monoclinic unit cells. The first is analogous to the widely accepted hemihydrate structure from Bezou *et al.* (1995), which is monoclinic because of a slight distortion of the trigonal lattice, *e.g.* by a shift in the positions of the water O atoms. Structure refinement in this cell was only possible using a program written by Bräu (2009) and Weiss & Bräu (2009), and treating the crystal as the racemic twin of a threefold twin. The second possible monoclinc cell is similar to the calcium sulfate hemihydrate structure found by Freyer *et al.* (1999). This hemihydrate formed a superstructure because of the partial substitution of calcium ions by two sodium ions. Refinement of both crystal structures was possible, but unfortunately it lead to negative anisotropic displacement parameters for several atoms in both cases.

A more detailed examination of the trigonal diffraction space ($2a = 2b$ = 14.1778 Å and $2c$ = 13.4262 Å) for extinction laws resulted in the discovery of very weak reflections with indices $l = 3n$ [normally (for the diffraction pattern of

[2] Supplementary data for this paper are available from the IUCr electronic archives (Reference: SN5102). Services for accessing these data are described at the back of the journal.

$CaSO_4 \cdot 0.5H_2O$) in (00l) in the small unit cell only reflections $l = 3n$, identical to $l = 6n$ in the large unit cell, are present]. In contrast to calcium sulfate hemihydrate, for calcium selenate subhydrate these reflections are not equal to zero. Thus, a screw axis 3_1 or 3_2 should be present. Possible space groups are $P3_1$, $P3_2$, $P3_121$ and $P3_221$ in the trigonal crystal system.

Structure solution by direct methods in these space groups resulted in a successful refinement for the space group $P3_2$. As a consequence of a high Flack parameter, the structure was refined as a racemic twin. *PLATON* (Spek, 2009) suggested the higher symmetry space group $P3_221$. Refinement in that group was successful. Hydrogen positions were located from the difference electron-density map and their distance to oxygen was restrained to 0.82 ± 0.02 Å. Information on the crystal and refinement are given in Table 1. The asymmetric unit is shown in Fig. 2. The coordinates and anisotropic displacement parameters can be found in the supplementary material.

The formula resulting from the structure solution is $CaSeO_4 \cdot 0.625H_2O$, in agreement with the water content determined by thermal analysis. Refinement of the structure against the data measured at 100 K was also successful. The unit-cell volume is decreased by 1.4% corresponding to a contraction of *ca* 0.5% of lattice parameters *a*, *b* and *c*. No phase transition was observed.

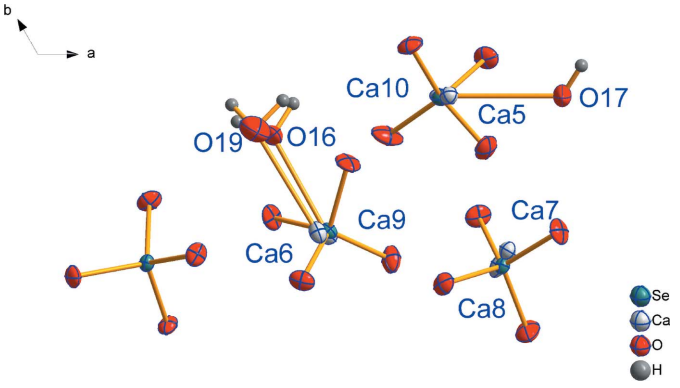

Figure 2
The asymmetric unit of calcium selenate subhydrate; displacement ellipsoids are drawn at the 50% probability level.

2.3. Powder diffraction, Rietveld refinement and maximum entropy method (MEM)

For the refinement of the lattice parameters and to test the single-crystal structure obtained against the bulk of crystals, consisting of crystals too small for single-crystal diffraction, additional powder diffraction experiments were carried out.

X-ray powder diffraction data of calcium selenate subhydrate were collected at room temperature (293 K) in Debye–Scherrer mode at the X16C beamline at the National Synchrotron Light Source, Brookhaven National Laboratory. The sample was contained in a sealed lithium borate glass capillary with 0.5 mm diameter (Hilgenberg glass No. 50). X-rays of wavelength ~ 0.7 Å were selected by a double Si(111) monochromator. The wavelength and zero-point error have been calibrated using eight precisely measured peaks of the NBS1976 alumina standard. The diffracted beam was analyzed by reflection from a Ge(111) crystal before a NaI scintillation detector. Data were taken in steps of 0.005° 2θ at a scanning speed of 8.0 s per step in the range 1–55°. The sample was spun to obtain better particle statistics. All data were normalized for storage ring-current decay by an ionization chamber monitor.

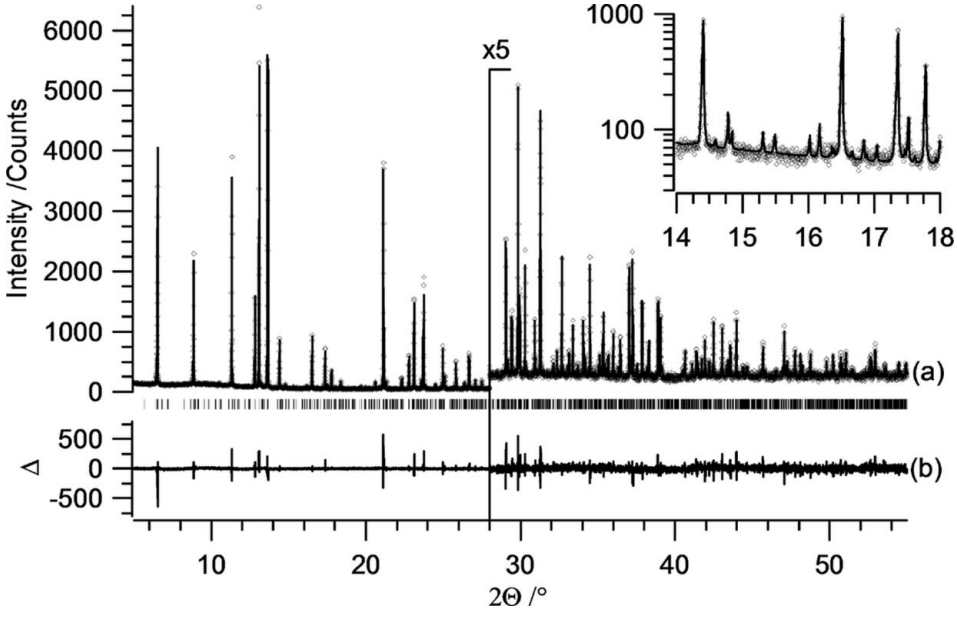

Figure 3
Scattered X-ray intensities of calcium selenate subhydrate at ambient conditions as a function of the diffraction angle 2θ. The observed pattern (diamonds) measured in Debye–Scherrer geometry, the best Rietveld fit profiles (line) and the difference curve between the observed and the calculated profiles (below) are shown. The high-angle part starting at 28° 2θ is enlarged for clarity. The inset shows the 2θ range from 14 to 18° on a logarithmic scale, thus visualizing small superstructure reflections.

For Rietveld refinement (Rietveld, 1969), the programs *TOPAS* (Bruker, 2007) and *JANA*2006 (Petříček *et al.*, 2006) were used. The peak profiles and precise lattice parameters of the powder pattern of calcium selenate subhydrate were first determined by a LeBail fit (Le Bail *et al.*, 1988). Refinement of the lattice parameters resulted in the values $a = b = 14.1681$ (2), $c = 13.4241$ (2) Å and $V = 2333.678$ Å^3.

Starting values for the atomic coordinates and the temperature factors were taken from the previous single-crystal investigation. For the final Rietveld refinement, all profile and lattice

Table 2
Details about the maximum-entropy computations.

The grid (pixels)	144 × 144 × 144
Algorithm	Sakata–Sato
Initial electron density	Flat
Constraints	F_2
$F(000)$	2184
Range of h, k, l	$0<h<18$ $-15<k<0$ $0<l<17$
R	0.0868
wR	0.0805
N_{pix} (unit cell/asymmetric unit)	2 985 984/995 328
No. of F constraints (input/expanded)	2093/12 350

parameters, an isotropic displacement factor and atomic positions of the heavy scattering atoms selenium and calcium were subjected to refinement. Despite the use of Debye–Scherrer geometry, a slight problem with preferred orientation was observed, which could be corrected by introducing symmetry-adapted fourth-order spherical harmonics into the refinement process. The diffraction pattern of $CaSeO_4{\cdot}0.625H_2O$, measured for Rietveld refinement, as well as the best Rietveld fit of the profile and the difference curve between both is shown in Fig. 3. The reliability factors for all reflections were $R_{wp} = 0.102$, $R_p = 0.084$, $R(F^2) = 0.066$ and $S = 1.48$.

Refinement of the oxygen positions of the water molecules was not possible with the Rietveld method. In order to independently confirm the correctness of the crystal structure for the bulk, particularly the position and amount of the interstitial water molecules, the maximum-entropy method (MEM) was applied since it allows for a very accurate reconstruction of the electron-density distribution from the experimental diffraction data.

As a starting point, the real and imaginary parts of the observed structure factors of the crystal structure found from the single-crystal experiment and refined with Rietveld were used. These structure factors were obtained using the program *JANA*2006 (Petříček *et al.*, 2006). The reliability factors for all reflections after the fit were $R_{wp} = 0.111$, $R_p = 0.0892$ and $S = 1.58$. These structure factors were used as input data to determine the electron-density distribution in the unit cell and locate the atoms using the program *BayMEM* (van Smaalen *et al.*, 2003). Atomic positions were localized from the map of electron-density distributions using the program *EDMA* (Palatinus & van Smaalen, 2005). Details for the maximum-entropy computations are given in Table 2.

The atomic positions obtained by the maximum-entropy method lie within 0.001 Å from those obtained after structure refinement of the single-crystal data, nicely confirming the validity of the single-crystal structure for the bulk sample. The electron density of the noise level is 20 times lower than the weakest density of the atoms from the structure. Such a large difference between maxima corresponding to atoms and noise indicate that all atoms were found.

3. Results and discussion

3.1. Characterization of calcium selenate subhydrate

A pure phase of calcium selenate subhydrate could be obtained from the hydrothermal conversion of calcium selenate dihydrate at 463 K. The X-ray powder diffraction pattern shows the same reflections as the only existing reference, $CaSeO_4{\cdot}0.5H_2O$ (JCPDS No. 16-481), and very weak additional reflections, which are not reflections of $CaSeO_4{\cdot}2H_2O$ (JCPDS No. 40-235) or $CaSeO_4$ (JCPDS No. 16-478).

Additional investigations showed that pure subhydrate crystallizes from supersaturated solutions under hydrothermal conditions at temperatures above 453 K, while at temperatures up to 433 K the selenate gypsum (calcium selenate dihydrate) is the solid phase. The hydrothermal conversion of sulfate gypsum is the standard procedure for the industrial production of α-calcium sulfate hemihydrate. However, while α-calcium sulfate hemihydrate can be obtained at temperatures around 393 K (literature reviewed in Freyer & Voigt, 2003) much higher temperatures are necessary to form the selenate subhydrate. The β-form of calcium sulfate hemihydrate is produced by dry heating of gypsum ('calcination'). However, in accordance with Crichton *et al.* (2010) we could not isolate selenate hemi- or subhydrate in this way. Dry heating of selenate gypsum always led to anhydrous calcium selenate (JCPDS No. 16-478). The selenate subhydrate obtained under hydrothermal conditions rehydrated under ambient conditions to selenate gypsum within weeks, but could be kept at low relative humidity (see below).

Analogous to α-calcium sulfate hemihydrate, calcium selenate subhydrate obtained under hydrothermal conditions formed crystals in the shape of long, hexagonal needles. SEM pictures are shown in Fig. 4 (for comparison, SEM pictures of calcium sulfate hemihydrate can be found in Fig. 3 of Freyer *et al.*, 1999, and Fig. 78 of Freyer & Voigt, 2003).

Thermal analysis of calcium selenate subhydrate (Fig. 5)

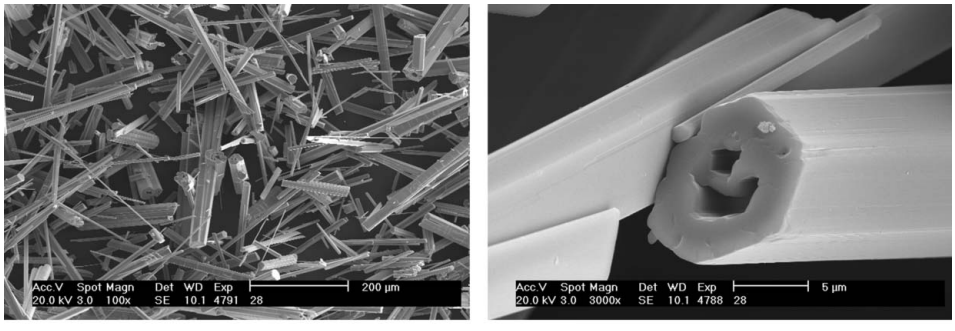

(*a*) (*b*)

Figure 4
SEM pictures of calcium selenate subhydrate; magnification (*a*) 100 and (*b*) 3000.

shows two endotherms at 382 and 429 K related to the loss of water in two steps. The total weight loss amounts to 5.8 ± 0.1% which is significantly more than the 4.7% consistent with the formula $CaSeO_4 \cdot 0.5H_2O$. Instead, the results suggest a water content of 0.63 ± 0.02 mol per mol of calcium selenate. Based on a water content of 0.63 mol, the first and second endothermic peaks can be assigned to the loss of 0.13 and 0.5 mol of water. This clearly shows that during the dehydration of the calcium selenate subhydrate, calcium selenate hemihydrate with an exact water content of 0.5 mol of water is formed as an intermediate phase. However, until now our attempts to obtain pure selenate hemihydrate from the subhydrate have not been successful. The water content remained the same even after heating the subhydrate for several days at 323 K or keeping it at 303 K over saturated LiCl or LiBr solution at a relative humidity of 7–11% for 2 months.

The results of the thermal analysis are contradictory to those of Fernández-González *et al.* (2006). They state that the selenate dihydrate loses 75% of its water content at temperatures of ∼ 443 K, thus forming the hemihydrate which remains stable up to the decomposition of the salt. However, it could also be possible that their intermediate phase actually was the subhydrate instead of the hemihydrate, since the corresponding dihydrate water loss of 10.9% instead of 12.3% would be consistent with the given thermogravimetric curves. We could not reproduce the observed stability of the hemihydrated phase at temperatures unusually high for hydrated salts. While our measurements were performed in an open crucible under nitrogen flow, the conditions from Fernández-González *et al.* (2006) are not specified. Differences in the measurement procedure could somewhat restrict the water release. However, it is surprising that it would almost completely suppress the formation of the anhydrous phase observed by others.

In the calcium sulfate system the hemihydrate exists at ambient conditions. The subhydrates are reversibly formed from the hemihydrate at high values of relative humidity only (> 40%; Bezou *et al.*, 1995; Kuzel & Hauner, 1987; Oetzel, 1999). The larger atomic radius of selenium compared with sulfur (+14%) seems to have such an influence on the crystal structure and the binding of the water molecules within the structure that the higher water content is preferred for the selenate at normal humidity, and the water release is shifted to higher temperatures compared with calcium sulfate hemihydrate (literature reviewed in Freyer & Voigt, 2003) and subhydrates (Holland, 1965; Paschke, 2011*a*).

FT-Raman spectra of selenate gypsum, selenate subhydrate and selenate anhydrite (the anhydrite obtained by dry dehydration of selenate gypsum at 573 K in the range 250–1000 cm^{-1}) are shown in Fig. 6.

Free selenate in solution has perfect T_d symmetry and exhibits four internal vibrations, $\nu_1(A1)$, the symmetric Se—O stretching mode at 833 cm^{-1}, $\nu_2(E)$, the symmetric SeO_4 bending mode at 335 cm^{-1}, $\nu_3(F2)$, the asymmetric stretching mode at 875 cm^{-1}, and $\nu_4(F2)$, the asymmetric bending mode at 432 cm^{-1} (Nakamoto, 1986).

The internal vibrations of the different calcium selenate phases differ significantly. Thus, Raman spectroscopy is a good

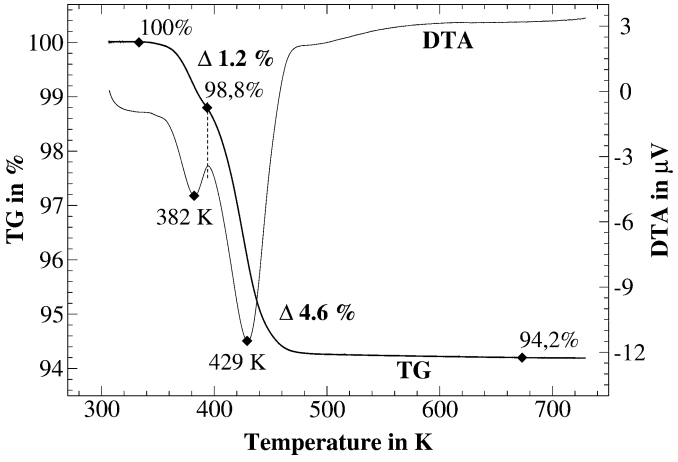

Figure 5
TG/DTA curves of calcium selenate subhydrate; heating rate 5 K min^{-1}.

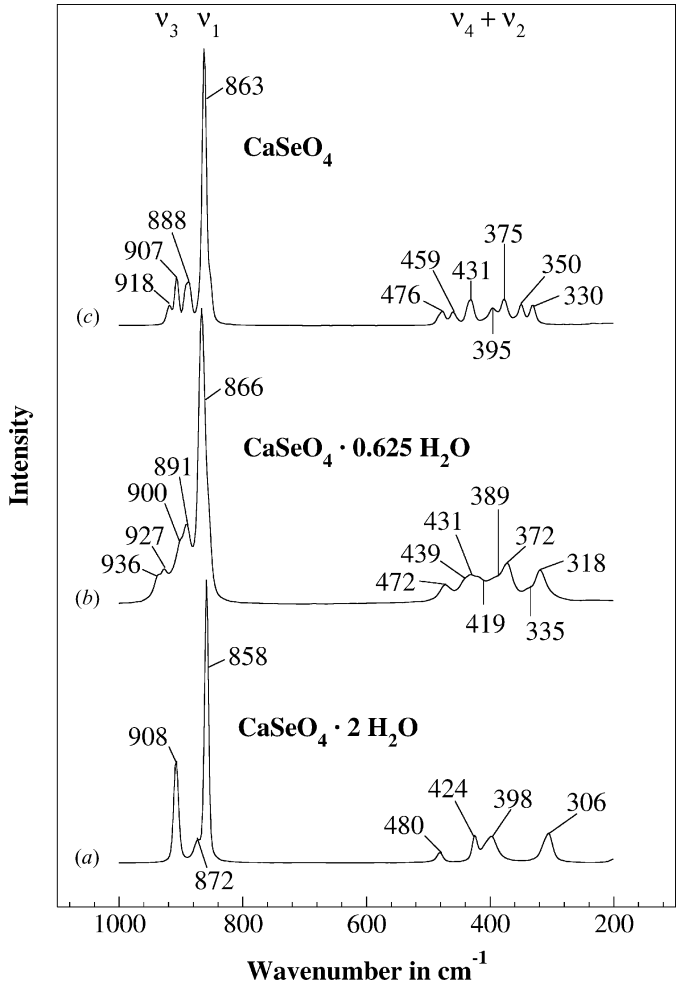

Figure 6
FT-Raman spectra of calcium selenate phases with different water contents; (*a*) calcium selenate dihydrate, (*b*) calcium selenate subhydrate and (*c*) calcium selenate anhydrite.

way to distinguish between the phases. Small contaminations (*e.g.* of nitrate contained in the starting material) can be easily identified by their strong vibrations at wavenumbers where there is no interference from selenate bands.

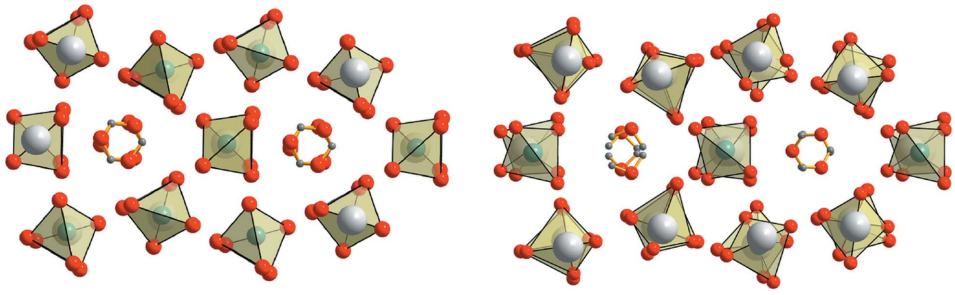

(*a*) (*b*)

Figure 7
Comparison between trigonal structures of calcium sulfate hemi- or subhydrate (identical with the substructure of calcium selenate subhydrate in the small trigonal unit cell, *a*) and the superstructure of calcium selenate subhydrate in the large trigonal unit cell (*b*), where the calcium and selenate ions do not form straight lines along **c**; calcium is indicated in grey, oxygen in red, hydrogen in dark grey and sulfate as well as selenate tetrahedra in yellow; the viewing direction is **c**.

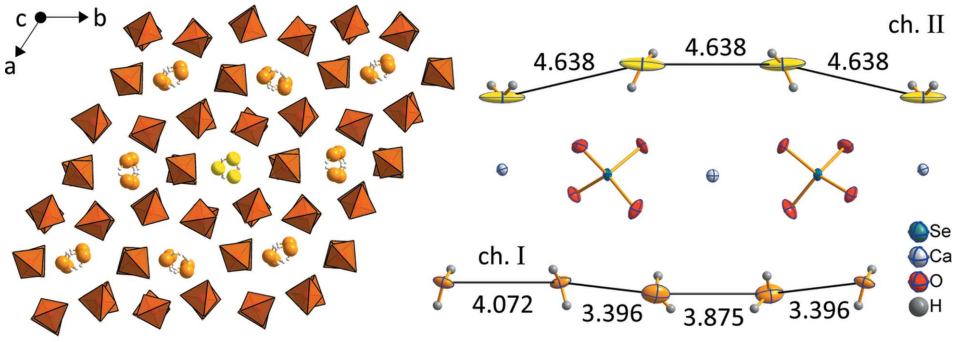

(*a*) (*b*)

Figure 8
Arrangement of the two types of water channels within the crystal structure of calcium selenate subhydrate (*a*) and arrangement of the water molecules within the different water channels with viewing direction perpendicular to **c** (*b*); the water in channel I is indicated in orange and in channel II in yellow; distances are given in Å.

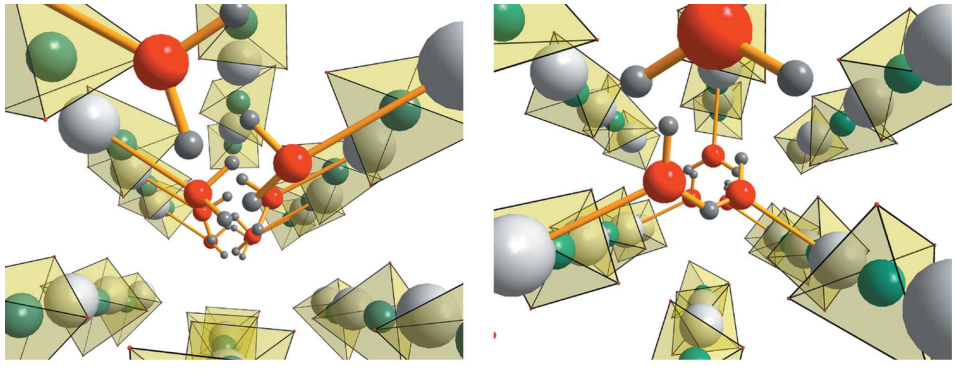

(*a*) (*b*)

Figure 9
Coordination of the water molecules within water channel I (*a*) and channel II (*b*) of calcium selenate subhydrate; **c** is the viewing direction. Calcium is indicated in grey, oxygen in red, hydrogen in dark grey and selenate tetrahedra in yellow.

3.2. Crystal structure of $CaSeO_4 \cdot 0.625H_2O$

The substructure or ionic framework of $CaSeO_4 \cdot 0.625H_2O$ is very similar to that of the calcium sulfate hemi- and subhydrate as well as the soluble anhydrite (AIII). The calcium ions and selenate tetrahedra alternate in sequence along the **c** direction, often simply expressed as calcium sulfate chains in the literature (as well as in the following text). These so-called chains, slightly shifted against each other parallel to **c**, form channels containing the water molecules. Discussions about the calcium sulfate hemi- and subhydrate structures are mainly on the subject of the arrangement of water molecules within the channels and the occupation of different water sites.

The substructure refined in the small trigonal cell (*cf.* §2.2) is almost identical to the trigonal structure solutions of the calcium sulfate hemi- and subhydrates (Gallitelli, 1933; Bushuev & Borisov, 1982*b*; Abriel & Nesper, 1993; Kuzel & Hauner, 1987; Abriel, 1983). Compared with these previous structures the new superstructure of $CaSeO_4 \cdot 0.625H_2O$, allows variation in the atomic positions of Ca^{2+} ions and the arrangement of SeO_4^{2-} tetrahedra and therefore more flexibility in the water channels. There are eight SeO_4^{2-} tetrahedra with different orientations, and the calcium and selenium atoms do not form a straight line in the **c** direction (Fig. 7).

Calcium is coordinated by eight selenate O atoms. Within one chain the two neighbouring selenate tetrahedra provide two O atoms each. The remaining four O atoms in the *ab* plane belong to selenate tetrahedra of the four surrounding chains. Additionally, five of eight calcium ions

are coordinated by one water oxygen.

Every water molecule is coordinated *via* oxygen to calcium and is stabilized by hydrogen bonds to selenate. Two different channels exist, with respect to the positions and the number of water molecules, in the structure of $CaSeO_4{\cdot}0.625H_2O$, as is evident from Fig. 8(*a*). One of the four channels (channel II) contains water molecules that are all related by the 3_2 axis. This channel is completely surrounded by channels of type I containing four independent water molecules each. In the small trigonal unit cell (see Fig. 7*a*) only one type of water channel is present analogous to the sulfate subhydrate structure models (Abriel, 1983; Kuzel & Hauner, 1987; Bushuev & Borisov, 1982*a*; Bezou *et al.*, 1995); also the water positions are statistically occupied which is not the case for the selenate subhydrate. Hence, the superstructure and the larger trigonal unit cell are caused by the ordering of two different water-channel structures I and II.

From Fig. 8(*b*) it can be seen that the channels differ in distances between the water molecules and in the anisotropic displacement ellipsoids. While the channel structure with four molecules (channel I) shows intermolecular distances of 4.072, 3.396, 3.875 and 3.396 Å, in the channel with three molecules (channel II) between the water molecules only one distance of 4.638 Å exists. In both channels the anisotropic displacement parameters of the water O atoms are high. In channel II the distribution of the water O atoms is elongated in the **c** direction.

The arrangement of water molecules within channel II is analogous to that of calcium sulfate hemihydrate. The water molecules are bonded to the three nearest calcium selenate chains along a threefold screw axis. Along one chain only every second calcium ion is coordinated. On the contrary, in channel I along one calcium selenate chain every calcium ion is coordinated by water oxygen, but only two of the three nearest calcium selenate chains are involved in the coordination (Fig. 9). Thus, in calcium selenate subhydrate a quarter of the calcium selenate chains are not coordinated by any water molecules.

Fig. 10 shows the electron-density calculated from powder X-ray experimental data for a projection of the unit cell [(001) plane with z corresponding to the maxima of the drawn atoms]. This figure clearly confirms the displacement of the structure units along the **c** direction and the different arrangement of the water molecules within the two channel types. The reduced symmetry of the water oxygen (O16, O19) in channel I with fourfold occupation can be recognized.

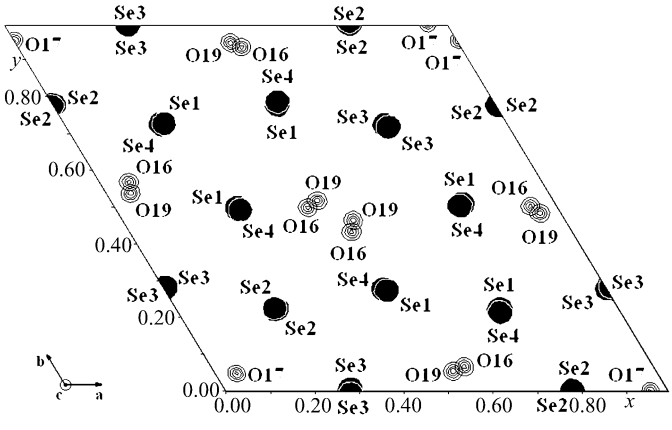

Figure 10
Electron-density map of calcium selenate subhydrate at ambient conditions in a projection along the *c* axis for different *z* values (corresponding to the maxima of the atoms drawn) calculated using the maximum-entropy method (after 99 000 cycles using *BayMEM*). The water molecules (O16, O17, O19) can be clearly seen.

4. Conclusion

Calcium selenate subhydrate, $CaSeO_4{\cdot}0.625H_2O$, can be prepared by hydrothermal synthesis starting from selenate dihydrate, in a way analogous to the production of autoclave gypsum (α-$CaSO_4{\cdot}0.5H_2O$) in the sulfate system.

The calcium selenate subhydrate crystals obtained are metastable at ambient conditions and transform within weeks or months in air into the dihydrate ($CaSeO_4{\cdot}2H_2O$). The subhydrate could not be obtained and isolated from the dihydrate by dehydration in air, which is the common way to prepare β-$CaSO_4{\cdot}0.5H_2O$ from gypsum ($CaSO_4{\cdot}2H_2O$). The selenate hemihydrate, $CaSeO_4{\cdot}0.5H_2O$, can only be monitored as the intermediate phase during the thermal dehydration of the dihydrate ($CaSeO_4{\cdot}2H_2O$) or subhydrate ($CaSeO_4{\cdot}0.625H_2O$).

By thermal analysis the hydrate water content of the calcium selenate subhydrate was determined to be 0.63 ± 0.02 mol per mol of $CaSeO_4$. The stoichiometry $CaSeO_4{\cdot}0.625H_2O$ was determined from the single-crystal analysis. The structure could be solved in a trigonal space group $P3_221$. More precise lattice parameters could be obtained by high-resolution synchrotron X-ray powder diffraction and Rietveld refinement [a = 14.1681 (2), c = 13.4241 (2) Å]. The atomic positions, especially those of the water O atoms within the channels of the $CaSeO_4$ matrix, could be confirmed by MEM.

The hydrate water content was found to be higher than the 0.5 mol expected according to the stoichiometry of bassanite, $CaSO_4{\cdot}0.5H_2O$. The higher water content of 0.625 mol is related to the formation of two types of structurally different water channels. Three of the four channels contain four water molecules, the fourth channel only three water molecules per unit cell (resulting in 15 water molecules per 24 calcium and sulfate ions). Depending on the number of water channels containing only three water molecules, selenate subhydrates with water contents of *e.g.* 0.54 (13/24), 0.58 (14/24), 0.625 (15/24) or 0.67 (16/24) could be derived.

Subhydrates with water contents between 0.5 and 0.8 mol of water are known for the calcium sulfate water system. However, while in the sulfate system the subhydrates only form at higher humidity, the selenate subhydrate exists under ambient conditions. While the hemihydrate, $CaSO_4{\cdot}0.5H_2O$, is widely accepted as being monoclinic, trigonal as well as monoclinc space groups and a statistical occupation of the water positions are suggested for $CaSO_4{\cdot}0.67H_2O$ (Bushuev & Borisov, 1982*a*; Kuzel & Hauner, 1987; Rinaudo & Boistelle,

1991; Bezou *et al.*, 1995). Considering the analogies between the $CaSO_4$–H_2O and $CaSeO_4$–H_2O systems the single-crystal X-ray diffraction experiments carried out in the current work suggest that a trigonal structure for calcium sulfate subhydrates with definite water positions is a good possibility.

Financial support by the Bundesministerium für Bildung und Forschung (BMBF), and the Fonds der Chemischen Industrie (FCI) is gratefully acknowledged. Special thanks go to Peter Stephens (SUNY at Stony Brook) for his help during data collection.

References

Abriel, W. (1983). *Acta Cryst.* C**39**, 956–958.
Abriel, W. & Nesper, R. (1993). *Z. Kristallogr.* **205**, 99.
Abriel, W. & Reisdorf, K. (1990). *J. Solid State Chem.* **85**, 23–30.
Berthold, C., Presser, V., Huber, N. & Nickel, K. G. (2011). *J. Thermal Anal. Calorim.* **103**, 917–923.
Bezou, C., Buisson, L., Mutin, J.-C. & Nonat, A. (1990). *C. R. Acad. Sci.* **311**, 1493–1498.
Bezou, C., Nonat, A., Mutin, J.-C., Noerlund Christensen, A. & Lehmann, M. S. (1995). *J. Solid State Chem.* **117**, 165–176.
Blessing, R. H. (1995). *Acta Cryst.* A**51**, 33–38.
Borrachero, M. V., Payá, J., Bonilla, M. & Monzó, J. (2008). *J. Thermal Anal. Calorim.* **91**, 503–509.
Bräu, M. F. (2009). Fortran source code. Personal communication.
Bruker (2005). *APEX*2, Version 2.2. Bruker AXS, Madison, Wisconsin, USA.
Bruker (2007). *TOPAS*, Version 4.1. Bruker AXS, Madison, Wisconsin, USA.
Bushuev, N. & Borisov, V. (1982*a*). *Russ. J. Inorg. Chem.* **27**, 341–344.
Bushuev, N. & Borisov, V. (1982*b*). *Russ. J. Inorg. Chem.* **27**, 344–347.
Crichton, W. A., Muller, H., Merlini, M., Roth, T. & Detlefs, C. (2010). *Mineral. Mag.* **74**, 127–139.
Fernández-González, A., Andara, A., Alía, J. M. & Prieto, M. (2006). *Chem. Geol.* **225**, 256–265.
Flack, H. D. (1983). *Acta Cryst.* A**39**, 876–881.
Freyer, D., Reck, G., Bremer, M. & Voigt, W. (1999). *Monatsh. Chem.* **130**, 1179–1193.
Freyer, D. & Voigt, W. (2003). *Monatsh. Chem.* **134**, 693–719.
Freyer, D. & Voigt, W. (2004). *Geochim. Cosmochim. Acta*, **68**, 307–318.
Gallitelli, P. (1933). *Period. Mineral.* **4**, 132–171.
Holland, H. (1965). PhD thesis, Bergakademie Clausthal, Germany.
Jacques, S. D. M., Gonzáles-Saborido, A., Leynaud, O., Bensted, J., Tyrer, M., Greaves, R. I. W. & Barnes, P. (2009). *Mineral. Mag.* **73**, 421–432.
Krüger, R.-R. & Abriel, W. (1991). *Acta Cryst.* C**47**, 1958–1959.
Kuntze, R. A. (1965). *Can. J. Chem.* **43**, 2522–2529.
Kuzel, H.-J. & Hauner, M. (1987). *ZKG*, **40**, 628–632.
Le Bail, A., Duroy, H. & Fourquet, J. L. (1988). *Mater. Res. Bull.* **23**, 447–452.
Meyer, J. & Aulich, W. (1928). *Z. Anorg. Allg. Chem.* **172**, 321–343.
Murat, M. & Comel, C. (1971). *Tonind. Ztg. Keram. Rundsch.* **95**, 29–35.
Nakamoto, K. (1986). *Infrared and Raman Spectra of Inorganic and Coordination Compounds*, 4th ed. New York: John Wiley and Sons.
Nishimura, T. & Hata, R. (2007). *Hydrometallurgy*, **89**, 346–356.
Oetzel, M. (1999). PhD thesis, RWTH Aachen, Germany.
Palatinus, L. & van Smaalen, S. (2005). *EDMA*. Laboratory of Crystallography, University of Bayreuth, Germany.
Paschke, I. (2011*a*). Master thesis, Institut für Anorganische Chemie, TU Bergakademie Freiberg, Germany.
Paschke, I. (2011*b*). In preparation.
Pedersen, B. F. & Semmingsen, D. (1982). *Acta Cryst.* B**38**, 1074–1077.
Petříček, V., Dušek, M. & Palatinus, L. (2006). *JANA*2006. Institute of Physics, Praque, Czech Republic.
Rietveld, H. M. (1969). *J. Appl. Cryst.* **2**, 65–71.
Rinaudo, C. & Boistelle, R. (1991). *J. Appl. Cryst.* **24**, 129–134.
Schmidt, H. (2011). In preparation.
Selivanova, N. M. & Shneider, V. A. (1958). *Nauch. Dokl.* pp. 664–666.
Selivanova, N. M. & Shneider, V. A. (1959). *Izv. Zav. Khim.* **2**, 651–656.
Sheldrick, G. M. (2008). *Acta Cryst.* A**64**, 112–122.
Simon, B., Pierrot, M. & Kern, R. (1963). *Bull. Soc. Fr. Miner.* **86**, 431–433.
Snyman, H. C. & Pistorius, C. W. F. T. (1963). *Z. Kristallogr.* **119**, 151–154.
Spek, A. L. (2009). *Acta Cryst.* D**65**, 148–155.
van Smaalen, S., Palatinus, L. & Schneider, M. (2003). *Acta Cryst.* A**59**, 459–469.
Weiss, H. & Bräu, M. F. (2009). *Angew. Chem. Int. Ed.* **48**, 3520–3524.